
A Guideline to Operational and Accidental Absorbed Dose Rates in the ESS Accelerator Tunnel

	Name	Role/Title
Owner	Lali Tchelidze	Safety Group Leader/Accelerator Division
Reviewer	Riccardo Bevilacqua	Scientist/Target Division
Approver	Mats Lindroos	Head of Accelerator Division

TABLE OF CONTENT

PAGE

1.	PURPOSE	4
2.	METHODOLOGY	4
3.	ASSUMPTIONS.....	4
4.	LIMITATIONS	4
5.	COMPUTER HARDWARE AND SOFTWARE	5
6.	CALCULATION INPUTS.....	5
7.	CALCULATIONS.....	6
7.1.	Full model simulation with 1 W/m uniform loss	6
7.1.1	Deposited power and absorbed doses along the LINAC	6
7.1.2	Deposited power and absorbed doses at various energies	8
7.1.3	Scoring results for X-Y cross sections at various energies.....	9
7.1.3.1	Deposited power for X-Y cross sections at various energies.....	10
7.1.3.2	Absorbed dose for X-Y cross sections at various energies	12
7.1.4	Particle spectra at various energies	14
7.1.4.1	Neutron spectra at various energies.....	14
7.1.4.2	Proton spectra at various energies	16
7.2.	Low energy (< 75 MeV) section simulation with 1 W/m uniform loss.....	17
7.2.1	Absorbed dose rates patterns in the low energy section	17
7.3.	High energy (2000 MeV) section simulation with 1W/m uniform loss.....	18
7.3.1	Abosrbed dose rates pttensrs in the high energy section	18
7.4.	Full 5 MW loss	19
8.	SUMMARY AND CONCLUSIONS	20
9.	GLOSSARY.....	21
10.	REFERENCES	21
	DOCUMENT REVISION HISTORY	21

LIST OF FIGURES

Figure 1 - Zoomed in cross section of the quadrupole and spoke cryomodule (as scored for 200 MeV).....	5
Figure 2 - Zoomed in cross section of the quadrupole pair and elliptical cryomodule (as scored for 500, 1000 and 2000 MeV)	5
Figure 3 - layout of the model axis, top view at x=0	6
Figure 4 - Deposited power maps for 50, 110 and 190 cm from the beam centre	7
Figure 5 - Absorbed dose maps for 50, 110 and 190 cm from the beam centre [Gy/h]	7
Figure 6 - Deposited power at ~ 200, 500, 1000 and 2000 MeV [mW/g]	8
Figure 7 – Dose absorbed at ~ 200, 500, 1000 and 2000 MeV [Gy/h]	9
Figure 8 - Power deposition around the quadrupole magnets [mW/g].....	10
Figure 9 - Power deposition around the accelerating cavities [mW/g].....	11
Figure 10 - Dose absorbed around quadrupole magnets [Gy/h]	12
Figure 11 - Dose absorbed hourly around the accelerating cavities	13
Figure 12 - Location of the spectra detectors	14
Figure 13 - Neutron spectra around the quadrupole at various distances from the beam at 200 MeV [1/Gev/cm ² /s]	14
Figure 14 - Neutron spectra around the quadrupole at various distances from the beam at 500 MeV [1/Gev/cm ² /s]	15
Figure 15 - Neutron spectra around the quadrupole at various distances from the beam at 1000 MeV [1/Gev/cm ² /s]	15
Figure 16 - Neutron spectra around the quadrupole at various distances from the beam at 2000 MeV [1/Gev/cm ² /s]	15
Figure 17 - Proton spectra around the quadrupole at various distances from the beam at 200 MeV [1/Gev/cm ² /s]	16
Figure 18 - Proton spectra around the quadrupole at various distances from the beam at 500 MeV [1/Gev/cm ² /s]	16
Figure 19 - Proton spectra around the quadrupole at various distances from the beam at 1000 MeV [1/Gev/cm ² /s]	17
Figure 20 - Proton spectra around the quadrupole at various distances from the beam at 2000 MeV [1/Gev/cm ² /s]	17
Figure 21 - Absorbed dose rates in low energy (< 75 MeV) sections [Gy/h]	18
Figure 22 – Absorbed dose rates in high energy (2000 MeV) sections [Gy/h]	19
Figure 23 – Absorbed dose rates for the 5 MW point beam loss [Gy/s]	20
Figure 24 – Absorbed dose rates for the 5 MW point beam loss [Gy/h]	20

1. PURPOSE

The purpose of this report is to provide operational and accidental absorbed dose rate values in the ESS accelerator tunnel. These values should be used as a guideline only and not as a requirement for equipment in the tunnel. The accelerator model version from November 2015 (available on the ESS cluster DMSC under /users/lali/ESS_Accelerator_Model/Nov10) was used with minor modifications as described in detail below.

The input information related to calculation model and assumptions was determined by the safety group of accelerator division of ESS, while the division of accelerator physics and technology, department of nuclear techniques and equipment, national center for nuclear research (NCBJ) in Poland has provided the results of the studies.

The work was supported by a PO nr 23000595 between the European Spallation Source ERIC and NCBJ.

2. METHODOLOGY

All simulations were performed with MARS Monte Carlo code [1][2][3].

3. ASSUMPTIONS

Normal operational 1 W/m proton beam loss was considered. This was derived from hands-on maintenance criteria for high intensity proton machines [5] and was adopted at ESS as a maximum allowable operational beam loss [6]. The beam loss was simulated as a homogeneous uniform loss around and across the vacuum beam pipe, with a shallow angle.

Additionally, a full point beam loss was considered for 2 GeV on a vacuum beam pipe as an accidental beam loss.

Information about the source terms, used materials and geometry models can be find in the report on Induced radioactivity studies in the ESS accelerator beam line components [6]. Data presented in this report was obtained during the same simulations as ones described there.

4. LIMITATIONS

1 W/m beam loss and a full 5 MW point beam loss were analysed.

Despite the fact that the model used for this task relies on the newest obtainable information about the ESS LINAC, it still varies from the actual machine. The biggest

missing parts in it are the accelerator components prior to the superconducting regions. Only quadrupoles are present in these areas. In terms of the dose maps, this might influence the results by making them more conservative – for these sections bulk metal components would act as an additional shielding, reducing the dose rates around the machine slightly.

5. COMPUTER HARDWARE AND SOFTWARE

- MARS15 version 1514, August 12-28, 2015

6. CALCULATION INPUTS

Four different simulations have been performed – full accelerator run, low energy section ($E < 75$ MeV), high-energy section and full beam loss of 5 MW.

Most scoring was done for the full LINAC simulation. Particle fluences were scored along the whole machine.

Smaller sections were also separated from the full model for finer scoring resolution. These regions span around the nominal energies (200, 500, 1000, 2000 MeV). Set of these regions cover only one quadrupole pair and following cryomodule (as seen in Figure 1 and Figure 2)

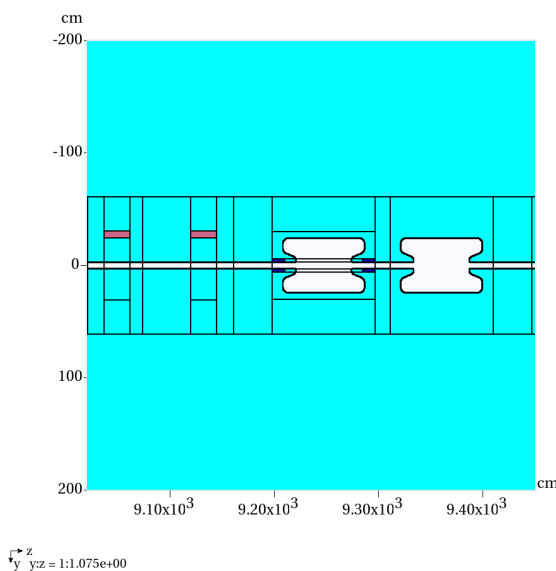


Figure 1 - Zoomed in cross section of the quadrupole and spoke cryomodule (as scored for 200 MeV)

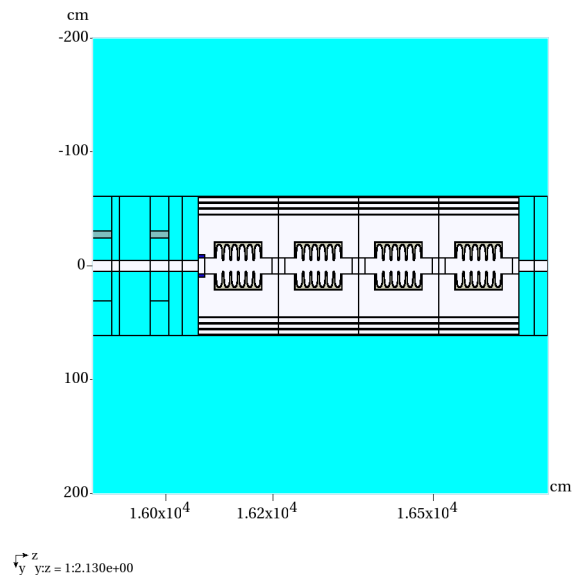


Figure 2 - Zoomed in cross section of the quadrupole pair and elliptical cryomodule (as scored for 500, 1000 and 2000 MeV)

Quantities scored in these regions are: PDT, DAB, DET, DEN, DEP, DRE, FLP, FLN (refer to Glossary).

When referring to the simulation dimensions and positions, x is the vertical axis, y is horizontal and z longitudinal along the machine - see the axis layout in Figure 3. $X=0$, $y=0$, $z=0$ is the middle of the beampipe ($x,y=0$) at the source position ($z=0$).

Additional scoring was performed around the quadrupoles and accelerating cavities in XY slices (– these results are not presented in this document, but they are available in the attached MARS output file and on request. A full list of scored histograms is available in the supporting file simulation_setup_long_model.xls.

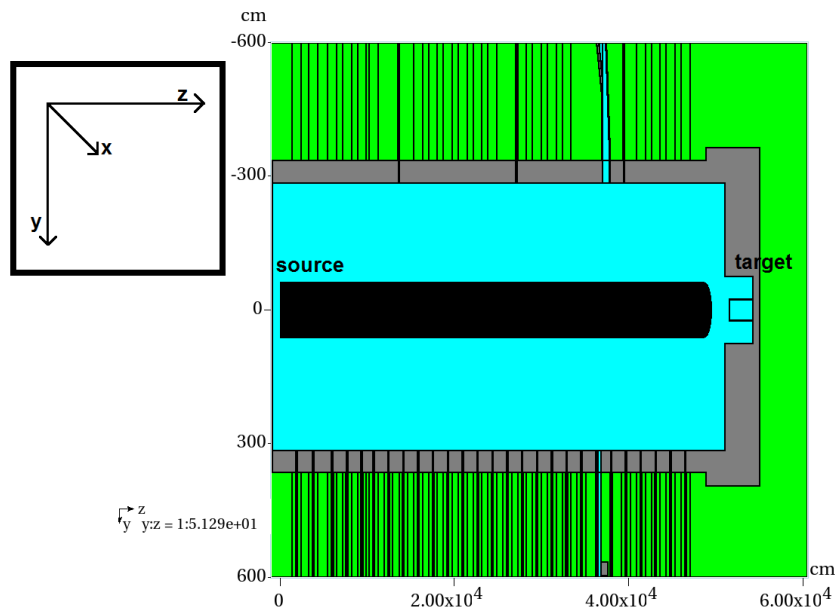


Figure 3 - layout of the model axis, top view at $x=0$

7. CALCULATIONS

All results, if not stated otherwise, are characterised with errors lower than 10% (usually much lower). Selected results for the prompt doses are shown below.

7.1. Full model simulation with 1 W/m uniform loss

7.1.1. Deposited power and absorbed doses along the LINAC

Figure 4 - Deposited power maps for 50, 110 and 190 cm from the beam centre presents deposited power along the whole ESS LINAC at different distances from the beam centre. Figure 5 presents the annual deposition in the present material at different distances from the beam centre.

Deposited power (and in result – dose) depends on the considered material. Much more power (for the particles and energy ranges considered in these simulation scoring) is deposited in bulk beampipe components with more interactions with the free particles than in the air filling the tunnel. This explains the spikes in the deposited power maps for the 50 cm away from the beam. Some scoring voxels contain the elements of the beamline, which absorb particles more than air which is the only material present at

depths 110 and 190 cm. One can consider those spikes as artefacts on the maps below present due to the resolution errors and only consider the figures clearly scoring the air deposition. For more precise results on components' power deposition one can refer to cross-section plots from 7.1.2 and 7.1.3.

Hourly absorbed doses (DAB) are of course consequent to the deposited power (PDT) but due to the inconvenient scaling (per second to per hour, factor 3600) they are presented here as well.

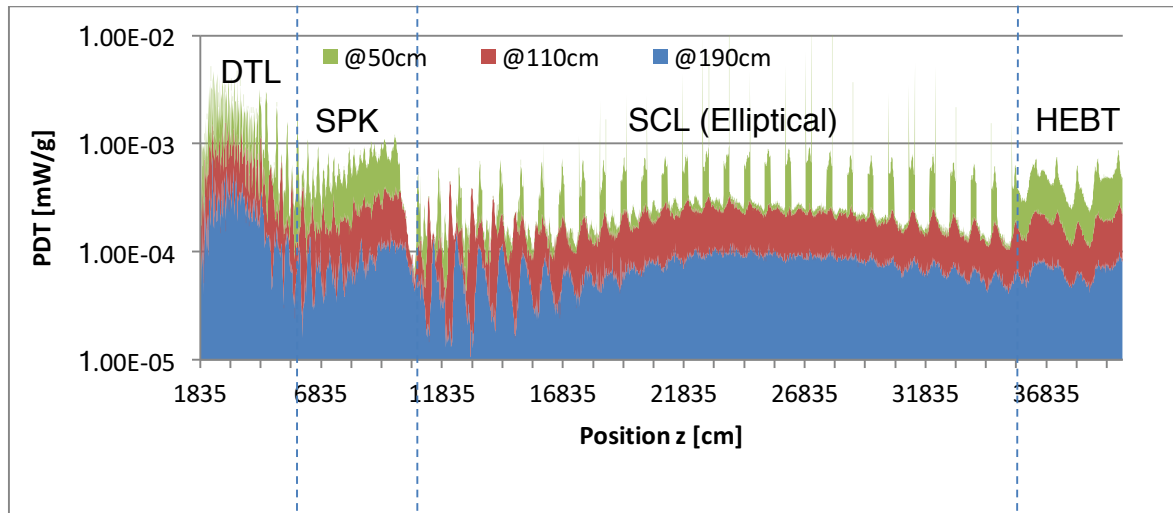


Figure 4 - Deposited power maps for 50, 110 and 190 cm from the beam centre

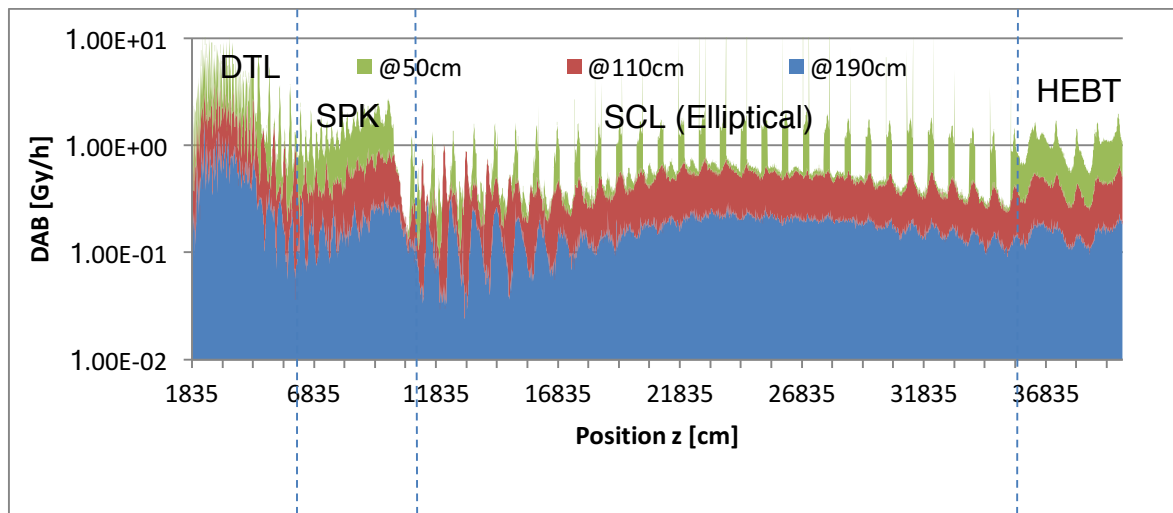


Figure 5 - Absorbed dose maps for 50, 110 and 190 cm from the beam centre [Gy/h]

Division between linac sections on Figures 4 and 5 are done roughly. DTL section corresponds to a partial drift tube linac, SPK corresponds to a spoke section of the linac, SCL (Elliptical) represents elliptical section of the linac and HEBT corresponds to a partial high energy beam transport region of the linac.

7.1.2. Deposited power and absorbed doses at various energies

Figure 6 shows the power deposited in the LINAC tunnel elements while Figure 7 presents the hourly dose absorption.

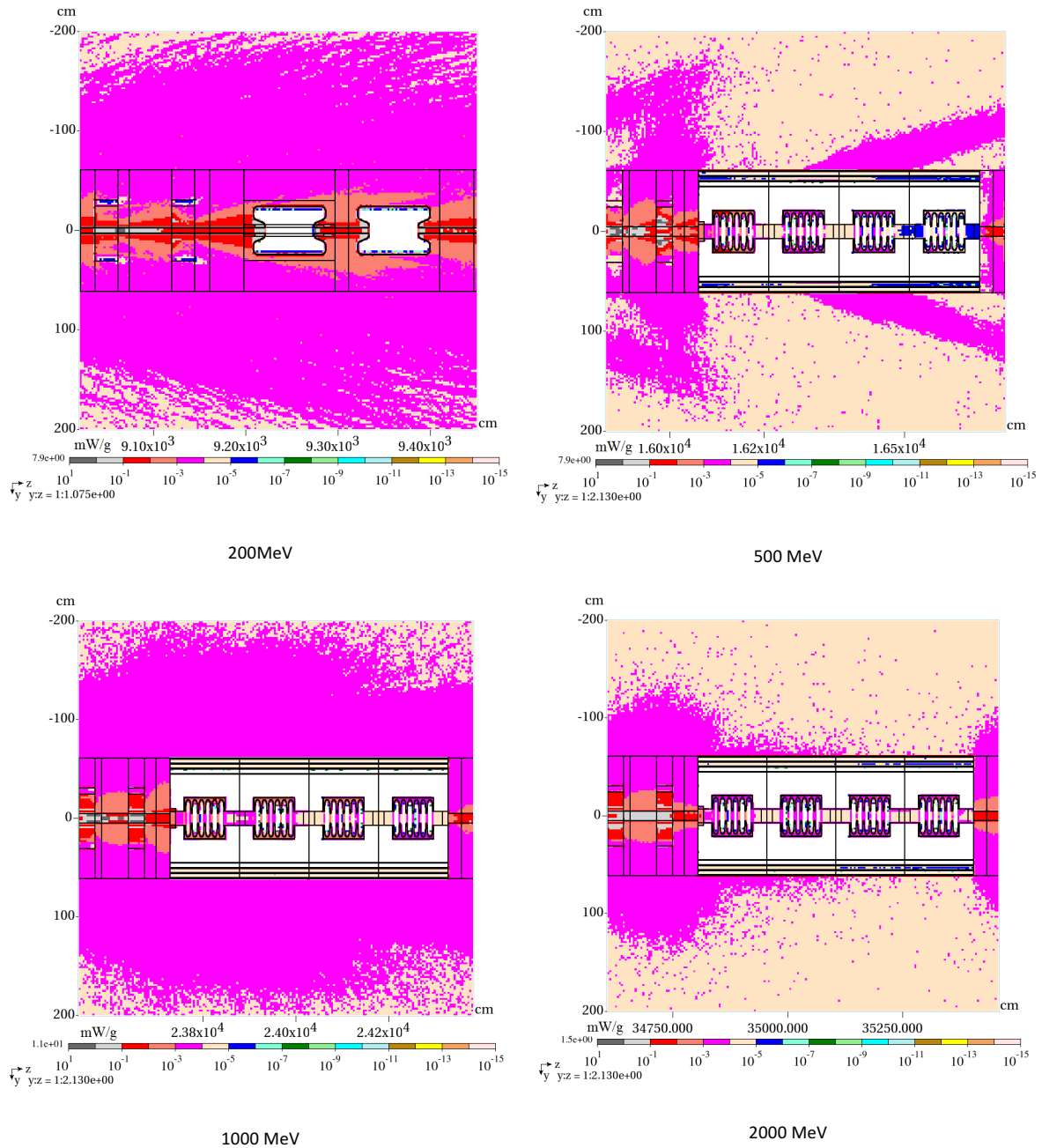


Figure 6 - Deposited power at ~ 200, 500, 1000 and 2000 MeV [mW/g]

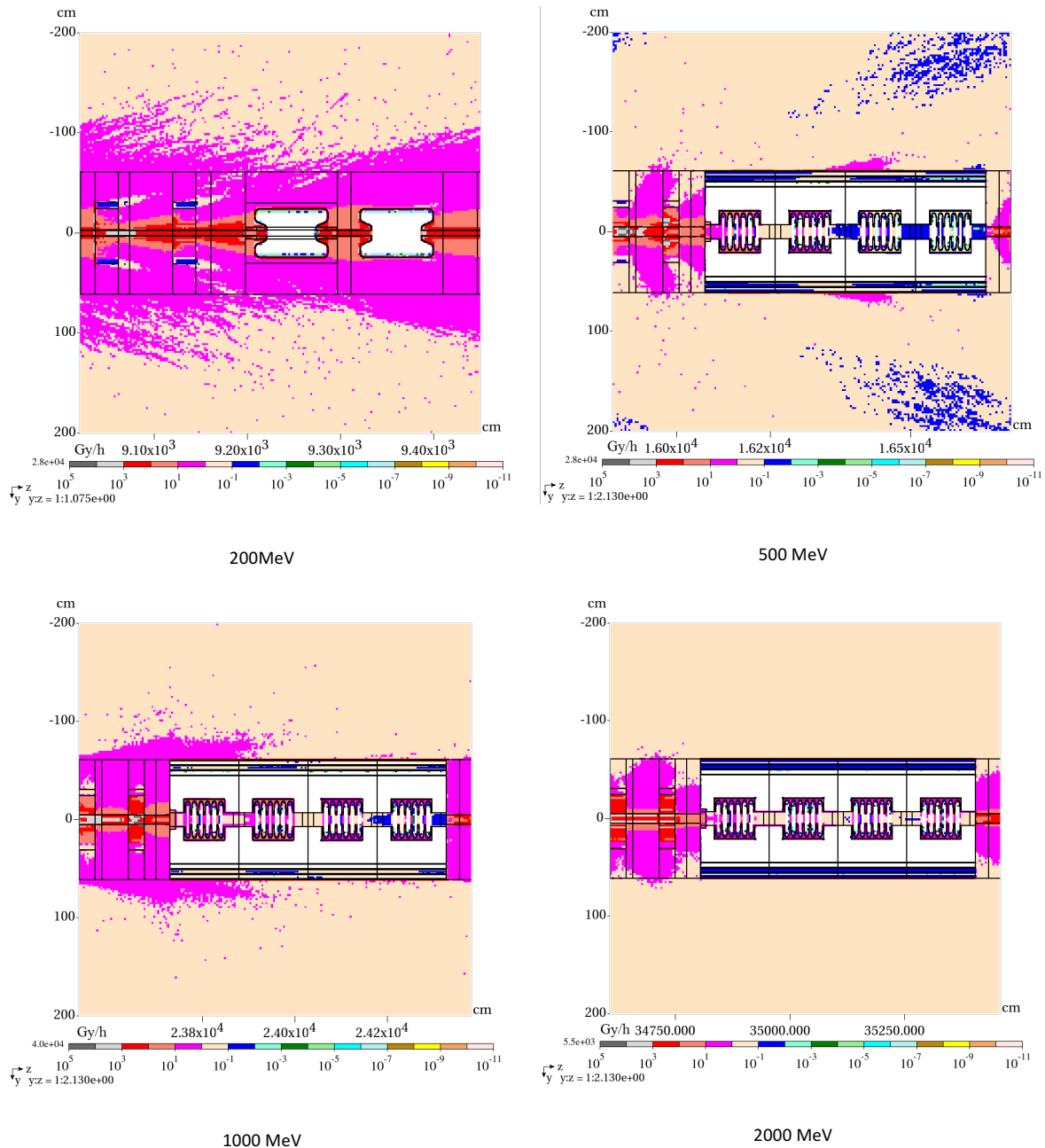


Figure 7 – Dose absorbed at ~ 200, 500, 1000 and 2000 MeV [Gy/h]

7.1.3. Scoring results for X-Y cross sections at various energies

Additional scoring in the X-Y plane was performed for two specific locations for each of the considered energies. One thin (10 cm) detector was located in the middle of the second quadrupole pair, while the other was located at the theoretical location for the cryomodule valve (beginning of the first spoke cavity and the middle of first cavity of the cryomodule).

Due to the thin nature of the detector some of these plots might have errors higher than desired 10%, but still give good approximation of the radiation conditions very close to the beampipe and stress on beampipe components.

7.1.3.1. Deposited power for X-Y cross sections at various energies

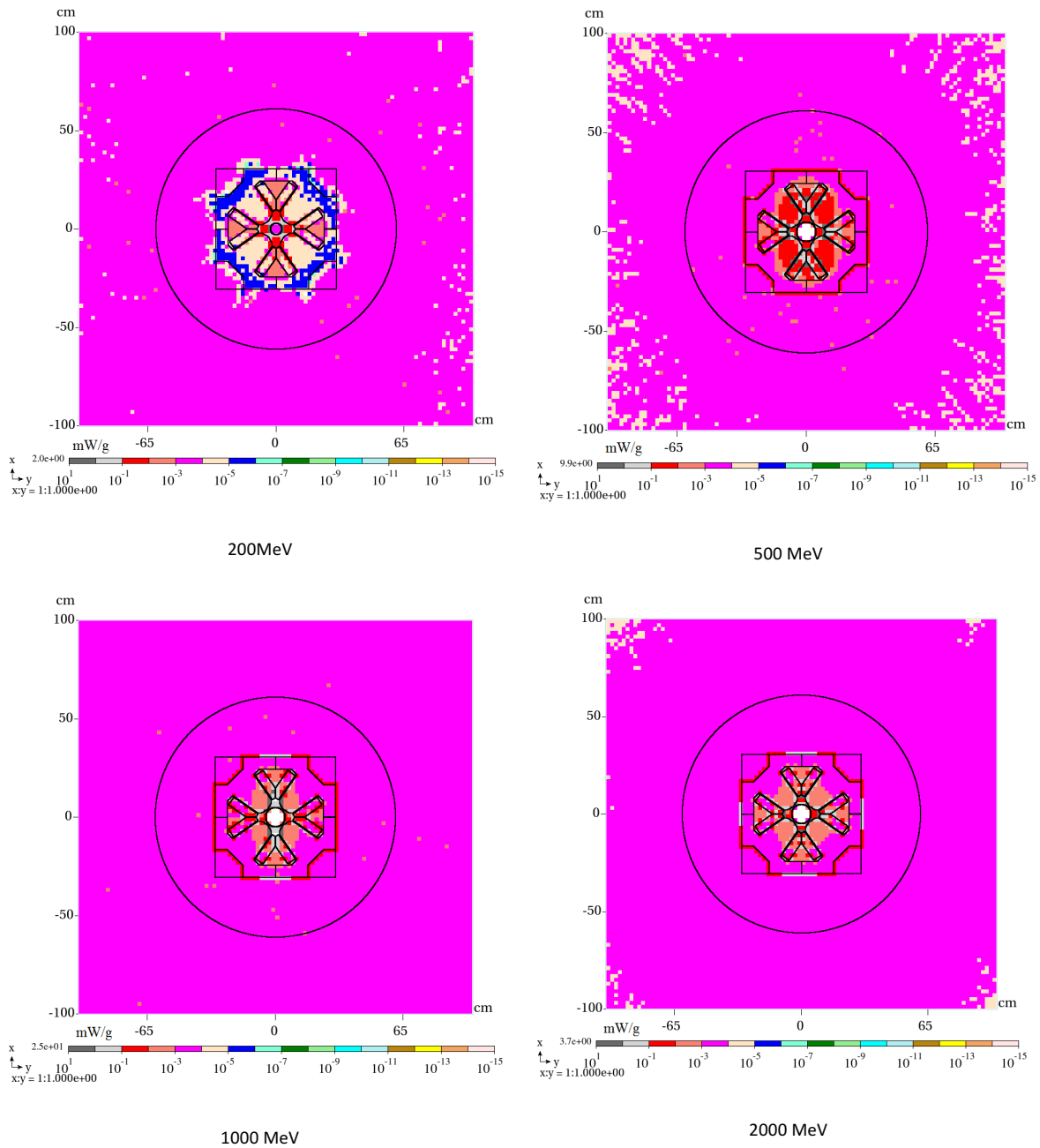


Figure 8 - Power deposition around the quadrupole magnets [mW/g]

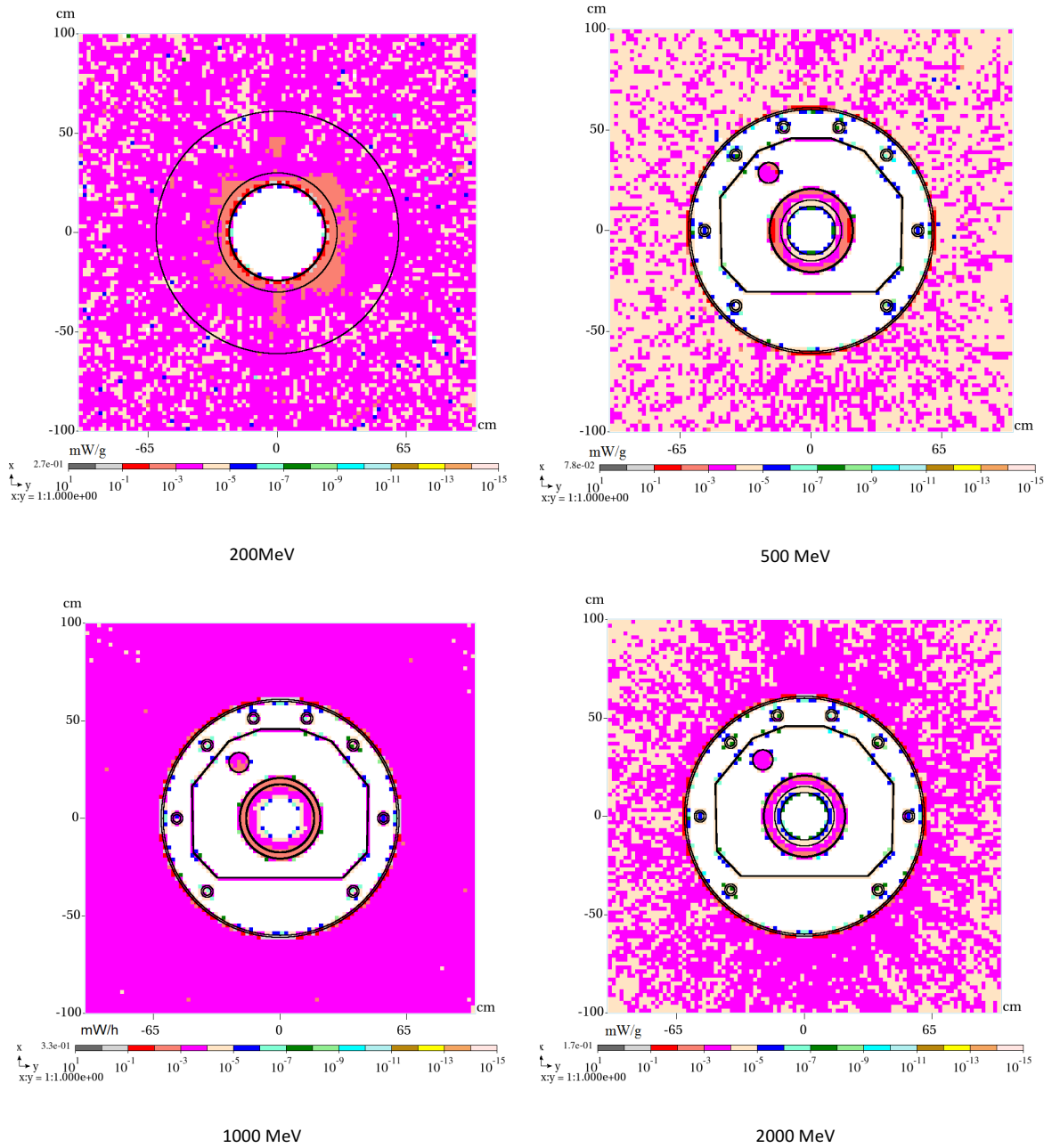


Figure 9 - Power deposition around the accelerating cavities [mW/g]

7.1.3.2. Absorbed dose for X-Y cross sections at various energies

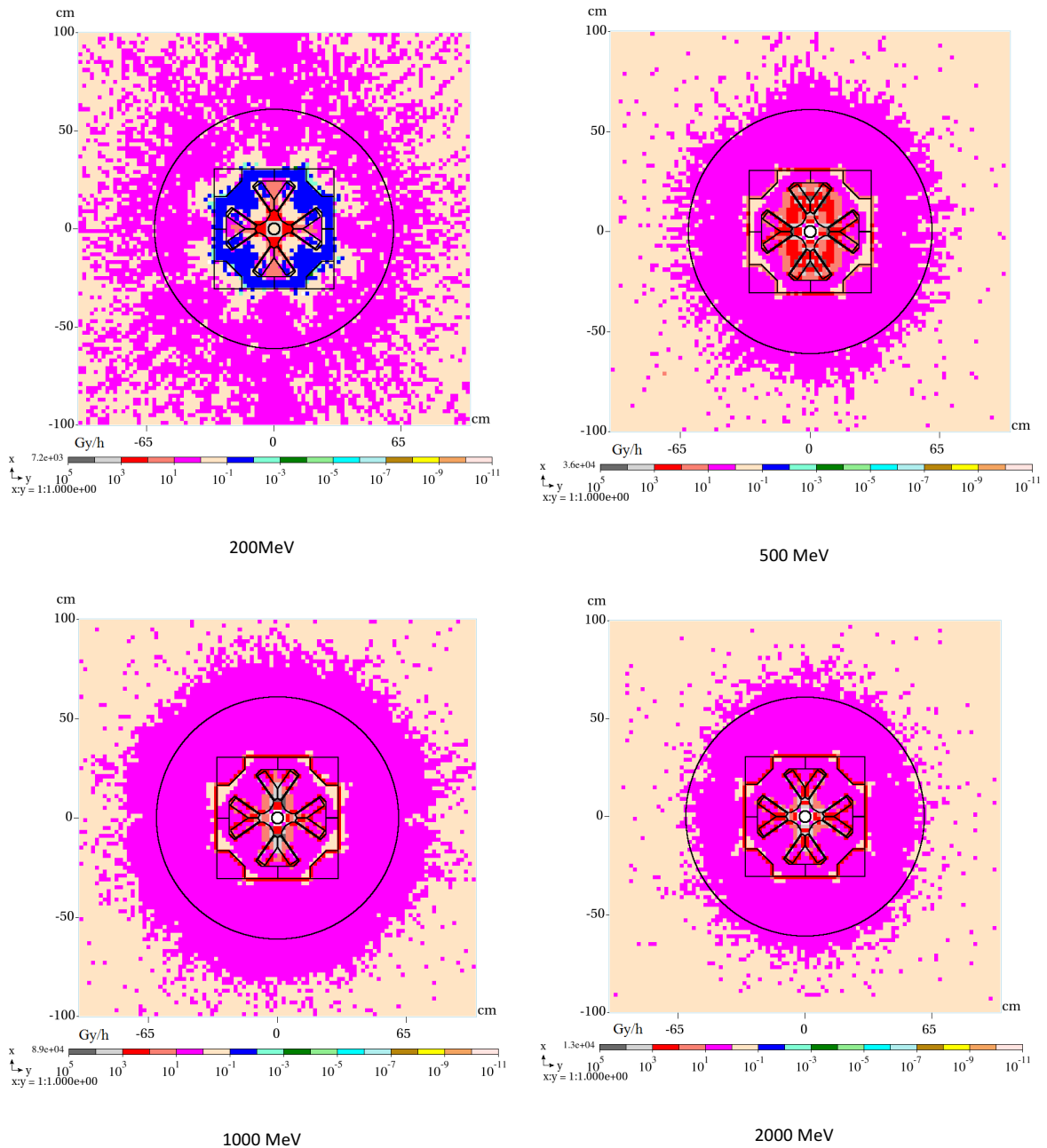


Figure 10 - Dose absorbed around quadrupole magnets [Gy/h]

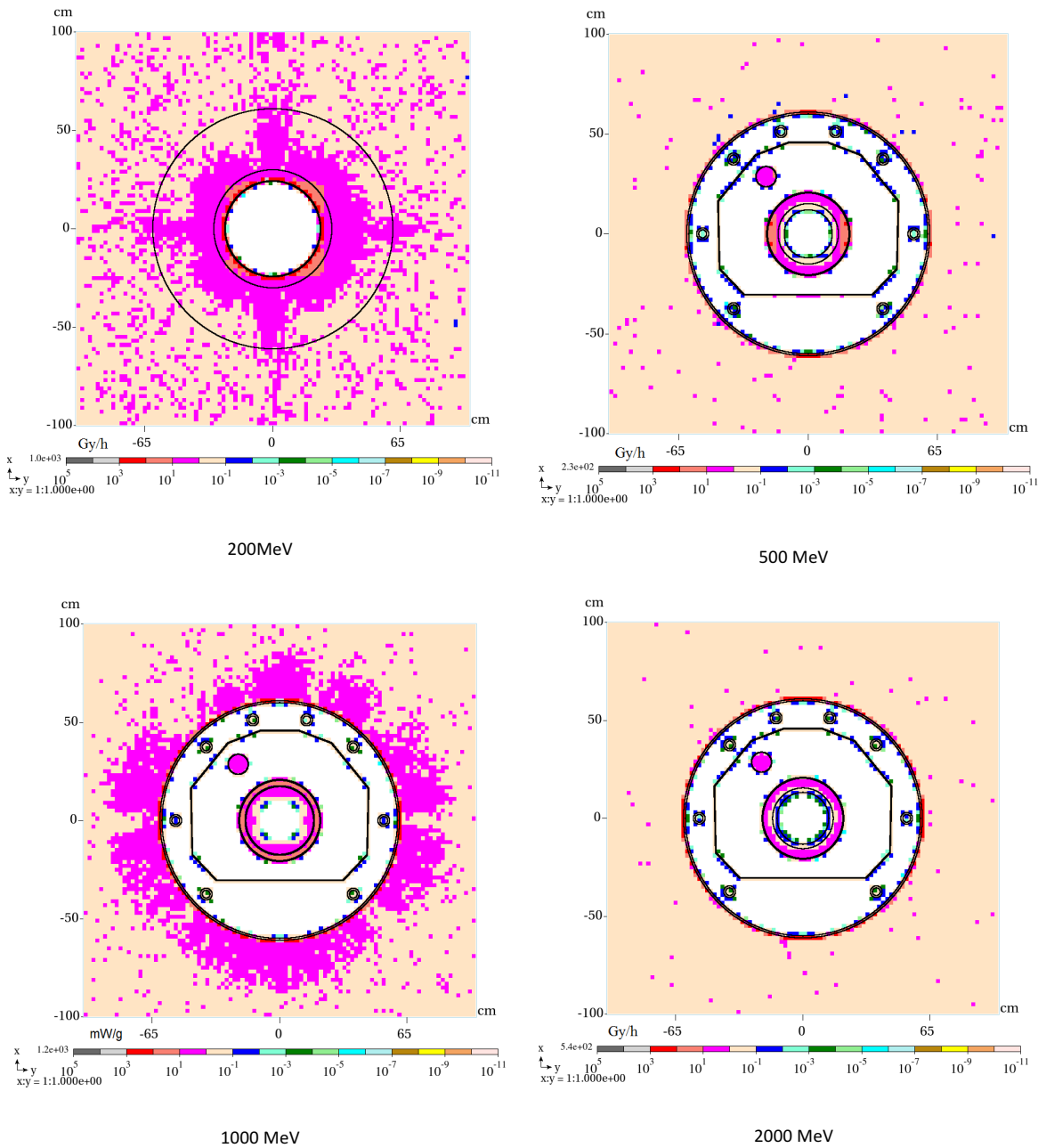


Figure 11 - Dose absorbed hourly around the accelerating cavities

7.1.4. Particle spectra at various energies

Spectra for neutrons and protons were measured for selected energies. Two locations of the spectrum detectors were considered: directly above the second quad of the pair (as in Figure 12) and above first cavity at given energy, similarly to the XY cross sections locations. As the generated spectra were similar for both cases, only the results for the quad detectors are presented here.

Spectra detectors are rectangular, with sides sized 20x20x10 cm (X Y Z).

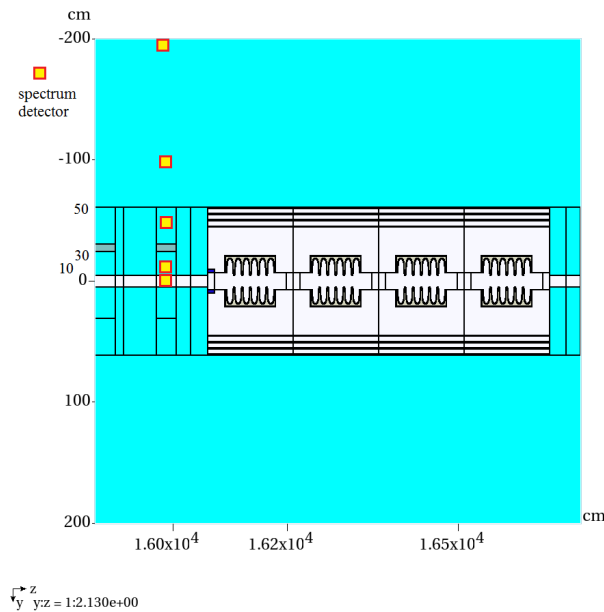


Figure 12 - Location of the spectra detectors

7.1.4.1. Neutron spectra at various energies

Neutrons @ 200 MeV, quad

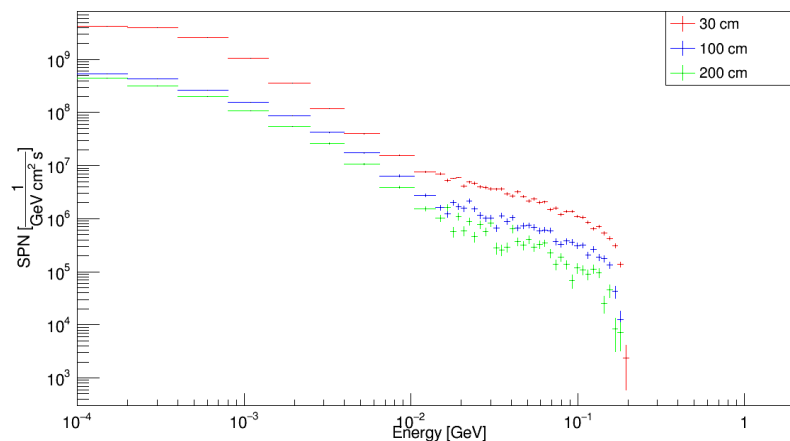


Figure 13 - Neutron spectra around the quadrupole at various distances from the beam at 200 MeV [1/GeV/cm^2/s]

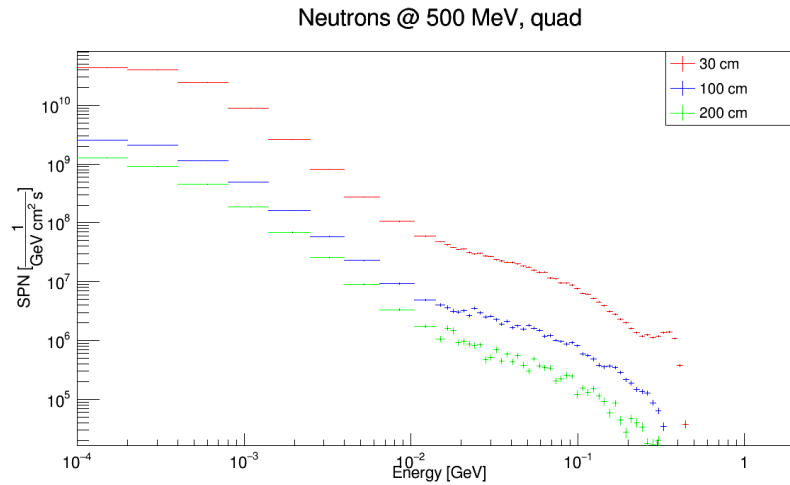


Figure 14 - Neutron spectra around the quadrupole at various distances from the beam at 500 MeV [1/GeV/cm²/s]

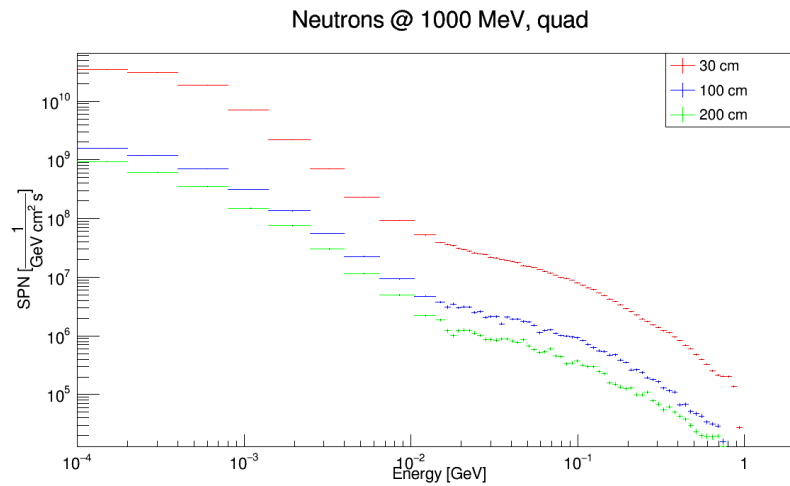


Figure 15 - Neutron spectra around the quadrupole at various distances from the beam at 1000 MeV [1/GeV/cm²/s]

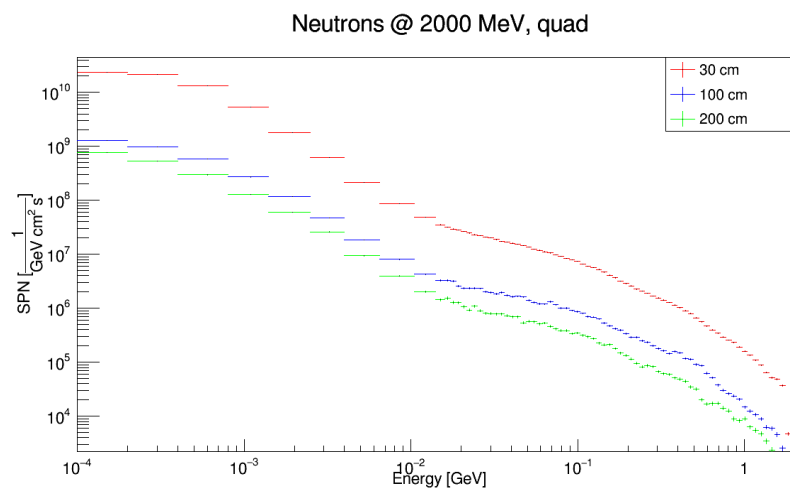


Figure 16 - Neutron spectra around the quadrupole at various distances from the beam at 2000 MeV [1/GeV/cm²/s]

7.1.4.2. Proton spectra at various energies

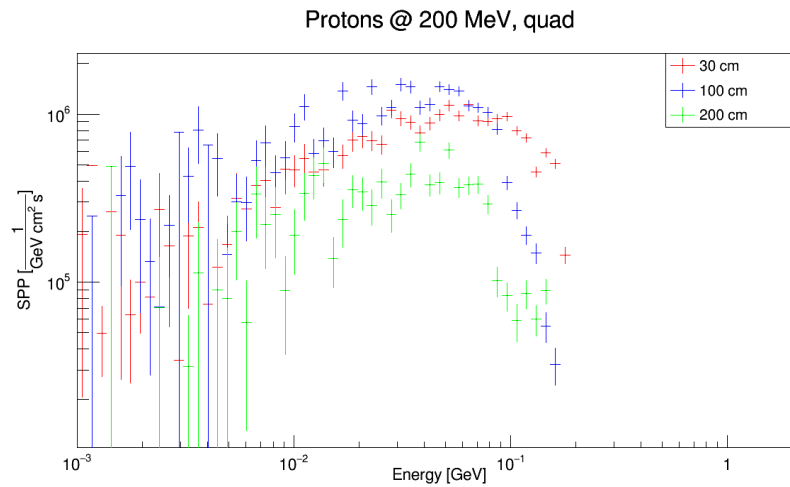


Figure 17 - Proton spectra around the quadrupole at various distances from the beam at 200 MeV [1/GeV/cm²/s]

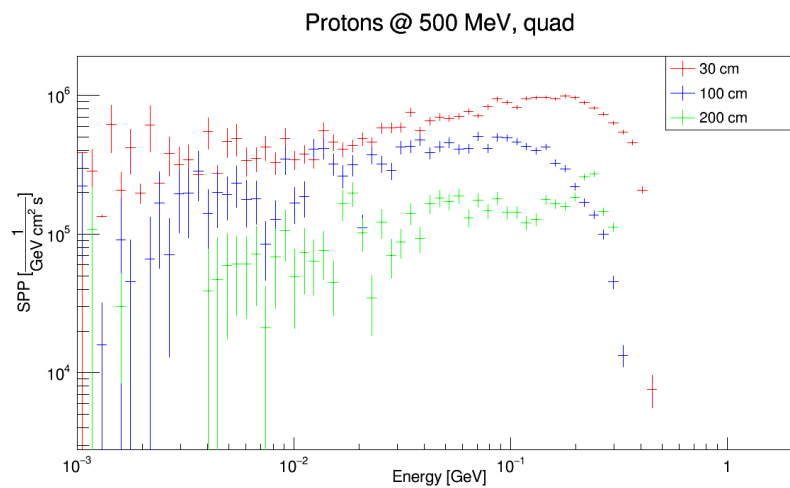


Figure 18 - Proton spectra around the quadrupole at various distances from the beam at 500 MeV [1/GeV/cm²/s]

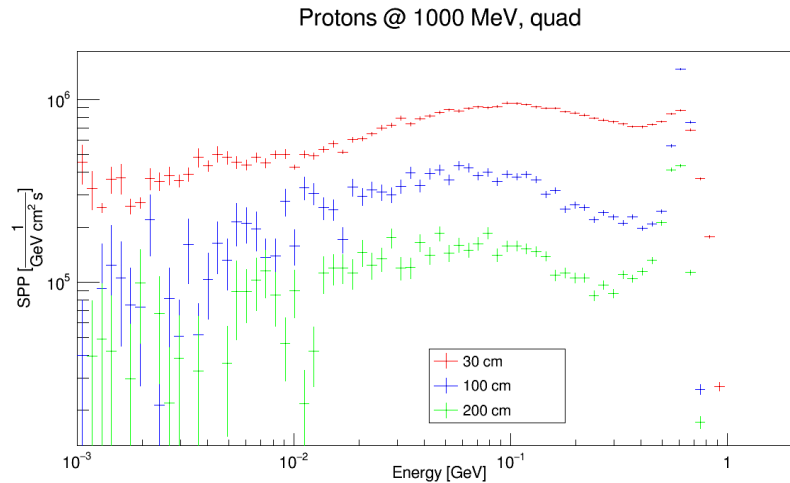


Figure 19 - Proton spectra around the quadrupole at various distances from the beam at 1000 MeV [1/GeV/cm²/s]

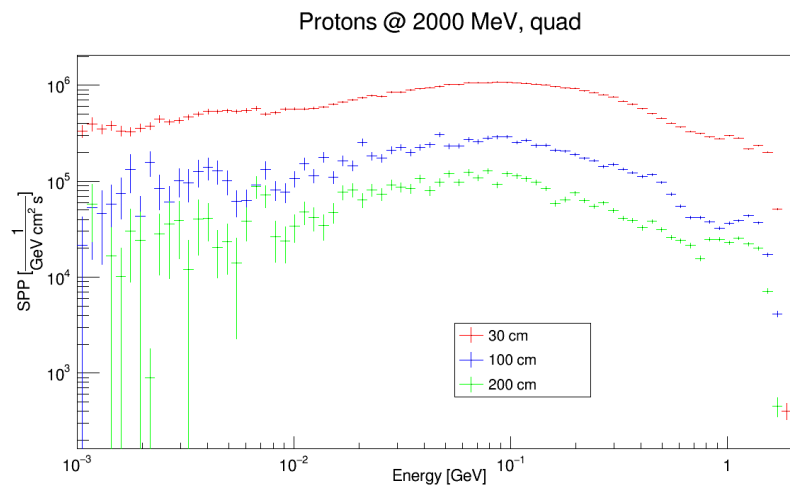


Figure 20 - Proton spectra around the quadrupole at various distances from the beam at 2000 MeV [1/GeV/cm²/s]

7.2. Low energy (< 75 MeV) section simulation with 1 W/m uniform loss

7.2.1. Absorbed dose rates patterns in the low energy section

Figure 21 shows total prompt dose rates in the low energy sections. Only half of the picture is present as the results are to a high extent symmetric.

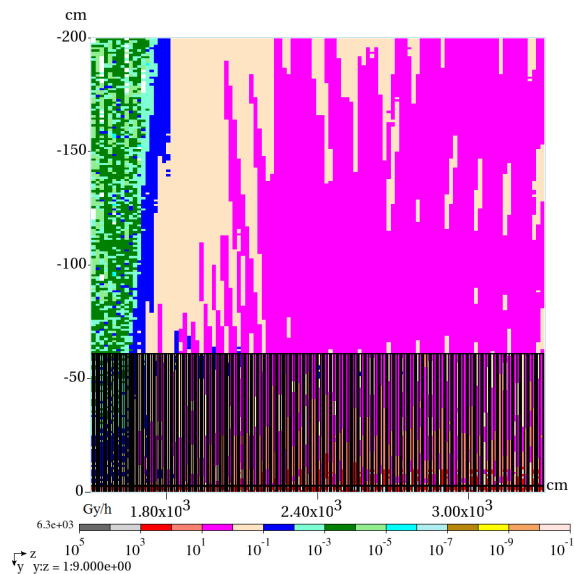


Figure 21 - Absorbed dose rates in low energy (< 75 MeV) sections [Gy/h]

7.3. High energy (2000 MeV) section simulation with 1W/m uniform loss

7.3.1. Absorbed dose rates patterns in the high energy section

Figure 22 shows absorbed dose rates in the low energy sections. Only half of the picture is present as the results are to a high extent symmetric.

One can immediately observe the sudden drop in dose rate close to the upstream sections compared to the previous results and following build-up. This is an artefact caused by a limited area of the high energy simulation – it starts at 354 m sharp. Particles lost before this position are not generated, therefore do not contribute to the doses of further regions, leading to their underestimation. As it seems from the plot, lost particles influence the downstream parts significantly for about 40 m from the place they were lost. This means that this simulation's results scored after about 400 m might be considered reliable.

The limitation in the simulation area was introduced to reduce the simulation time.

This simulation was not foreseen to score precisely the doses as it is a setup to score mainly air activation. However, it can be observed, that after 3-4 quadrupoles the doses stabilize and are equal to those scored in the full accelerator run.

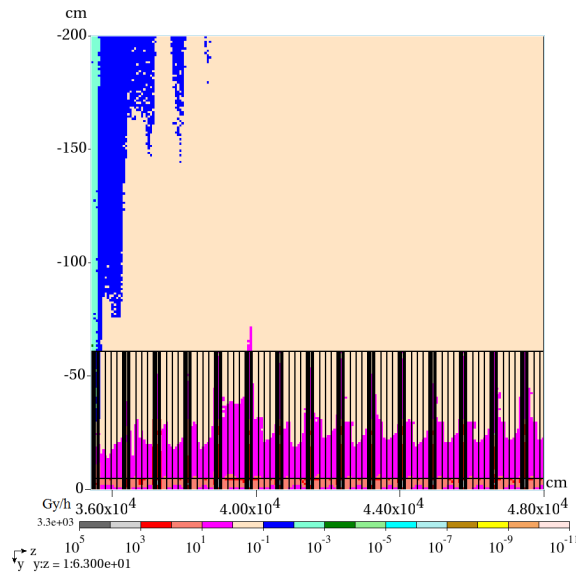


Figure 22 – Absorbed dose rates in high energy (2000 MeV) sections [Gy/h]

7.4. Full 5 MW loss

Figure 23 shows the absorbed dose rates during the full point beam loss at 2000 MeV in the upgrade section. One can observe that the particles ‘lost’ in the first quadrupole in fact travel few meters freely until they hit an aperture of the beampipe close to the next cryomodule. Figure 23 – Absorbed dose rates for the 5 MW point beam loss [Gy/s] shows the dose rate per second, while Figure 24 shows them hourly, which isn’t realistic, but can be helpful to realise how much higher the absorbed doses will be in comparison to the normal accelerator behaviour.

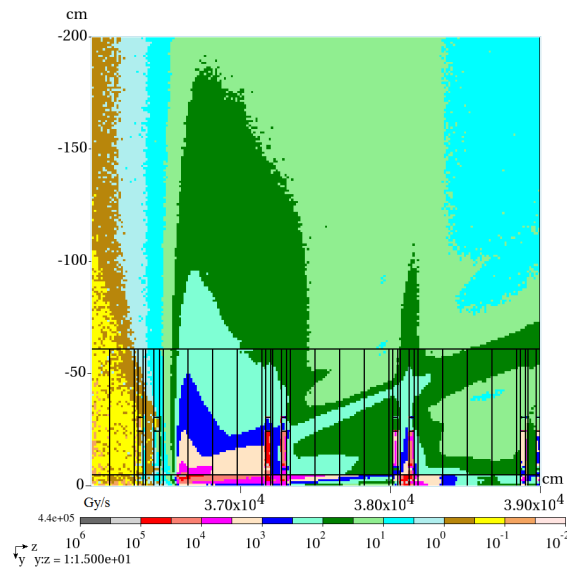


Figure 23 – Absorbed dose rates for the 5 MW point beam loss [Gy/s]

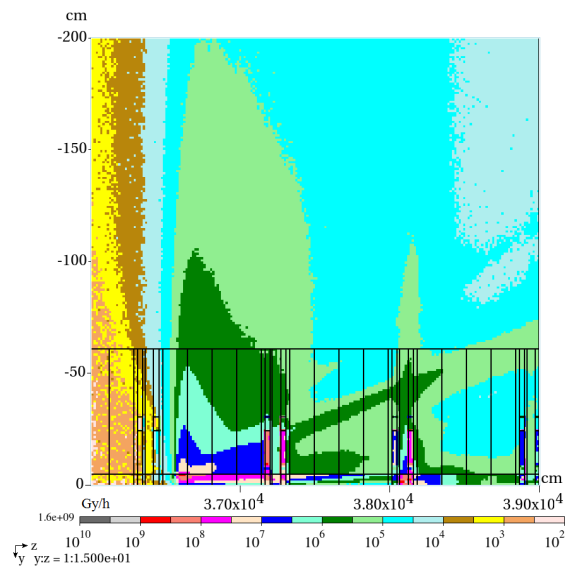


Figure 24 – Absorbed dose rates for the 5 MW point beam loss [Gy/h]

8. SUMMARY AND CONCLUSIONS

Operational and accidental absorbed dose rate values in the ESS accelerator tunnel were investigated and presented in this report. Presented values should be used as a guideline only and not as a requirement for equipment in the tunnel.

9. GLOSSARY

Term	Definition
ESS	European Spallation Source
A2T	Accelerator to Target
LINAC	Linear Accelerator
MC	Monte-Carlo
PDT	Power Density Total
DAB	Dose Absorbed
DET	Dose Equivalent Total
DEN	Dose Equivalent from Neutrons
DEP	Dose Equivalent from Protons
FLP	Proton Fluence
FLN	Neutron Fluence

10. REFERENCES

- [1] N. V. Mokhov, *The MARS Code System User's Guide*, Fermilab-FN-628 (1995)
- [2] N. V. Mokhov, S. I. Striganov, MARS15 Overview, in *Proc. of Hadronic Shower Simulation Workshop*, Fermilab, Sept. 2006 AIP Conf. Proc. 896, pp. 50-60 (2007)
- [3] N. V. Mokhov et al., *Prog. Nucl. Sci. Technol.* 4, 496 (2014)
- [4] <http://dx.doi.org/10.15669/pnst.4.496>; <http://www-ap.fnal.gov/MARS/>
- [5] O.E. Krivosheev and N.V. Mokhov, "Tolerable Beam Loss at High-Intensity Proton Machines", FERMILAB-Conf-00/192, 2000
- [6] ESS-0008351, ESS hands on maintenance conditions for ESS accelerator
- [7] ESS-0051492, Induced radioactivity studies in the ESS accelerator beam line components

DOCUMENT REVISION HISTORY

Revision	Reason for and description of change	Author	Date
1	First issue	Michał Jarosz, Lali Tchelidze	2016-07-11
2	Updated values in Figures 4 and 5	Michał Jarosz, Lali Tchelidze	2017-01-24

Document Type Report
Document Number ESS-0060208
Revision 3

Date May 12, 2017
State Released
Confidentiality Level Internal

Revision	Reason for and description of change	Author	Date
3	Added description of sections in Figures 4 and 5	Michał Jarosz, Lali Tchelidze	2017-05-10